2011 50th IEEE Conference on Decision and Control and
European Control Conference (CDC-ECC)
Orlando, FL, USA, December 12-15, 2011

Estimating the Speed and Motion Direction of Targets using a Model of the Turtle Retina

Bijoy K. Ghosh and Mervyn P. B. Ekanayake

Abstract— **In this paper we show how the velocity of a moving target across the visual field can be estimated using model of a turtle retina. The model of the retinal cells is the same as obtained earlier by the authors. Using the model, we show that the motion direction and the speed, of a target moving along a straight line, with constant speed, can be estimated in two steps. The speed can be estimated independently of the angle of the optical flow induced by the target motion. Using the speed, the retinal (model) response can be rescaled and the angle of optical flow (hence of the motion direction of the target) can be estimated independently of the speed.**

I. Introduction

Retina is the doorway to the visual system in any animal. Turtle retina are interesting due to many reasons, it has many types of cells, and are structurally different, for example from that of humans. In addition to the cells which are only sensitive to the intensity of the visual stimuli, some cells of the turtle retina are sensitive to both the intensity as well as the optical flow induced by the motion of objects incident on the visual field [1]. The cells which are only sensitive to the intensity of the visual stimuli are called intensity sensitive cells or simply 'A cells'. The cells which are sensitive to both intensity and the optical flow are called direction sensitive cells or simply 'B cells'. The cells can be of several kinds when we consider the receptor field structure [2]. The A cells could either be with an excitatory center and inhibitory surrounding (ON cells), or with an inhibitory center and excitatory surrounding (OFF cells). Here, excitatory means that cell will be inclined to produce more spikes when the input is incident on that region and inhibitory means that the cell will be inclined to lessen the rate of spikes it produces. The B cells are ON-OFF type, meaning that there is an inhibitory annulus sandwiched between an excitatory center and another excitatory annulus further away [1]. The same paper describes, in principle, that there are three types of B cells according to their direction preference: 180°, 40° and -75°. The A cells have a larger cell body size compared to B cells [2]. The distribution of the size of retinal ganglion cells and the spatial distribution of cells on the retina has been studied in detail in [3] and [4].

This paper is based upon work supported in part by the National Science Foundation under Grant No. 1029178. Any opinions, findings, and conclusions or recommendations expressed in this paper are those of the author(s) and do not necessarily reflect the views of the National Science Foundation.

Bijoy K. Ghosh and Mervyn P. B. Ekanayake are with Center for BioCybernetics and Intelligent Systems, Department of Mathematics and Statistics, Texas Tech University, Lubbock, TX 79409, USA. {bijoy.ghosh, mpb.ekanayake}@ttu.edu

The authors have developed a model of the turtle retinal cells as can be seen in [5], [6] and [7]. In [6] and [7], the authors discuss the application of the cell model to detect direction of motion incident on the visual space of the model retina. In this paper we use the same model cell to estimate the velocity of a moving target on the visual space.

A retinal cell is modeled as two synaptically coupled stages. The first stage is a cascade of filters, modeling the layers of rods and cones of the retina. The response of the filter cascade projects on to the second stage, which is a Hodgkin-Huxley spiking neuron model, as a synaptic input. We do not intend to describe the model of the retina in this paper since it is already reported. We refer to three publications [5], [6] and [7] mentioned above for the details of the cell model. The model accepts a movie of a moving light spot as the input stimulus and produces a train of spikes by each cell.

The cells on the turtle retina are distributed in a visual streak structure (see Fig. 1), as opposed to a fovea as in humans. When the cells of a retina are distributed in such a way that the highest density of cells are along a line, we call it a visual streak. On the other hand, if the cells are distributed about a maximum density point, we call it a fovea. We have chosen a patch sampled from the center of the retina for our simulation experiments.

The resulting spike trains corresponding to a particular input can be thought of as a counting process. In fact, we can model this counting process as a self exciting counting process (see [8], [9]). By pooling the several counting processes, it is possible to model the resultant process as

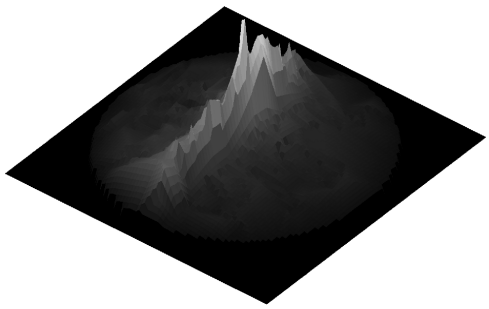

Fig. 1: Distribution of cells on the retina, lighter shade indicates a higher density. The retinal patch used for the analysis in this paper is a circular region, roughly one tenth the diameter of the retina and centered at the region with highest density.

978-1-61284-799-3/11/$26.00 ©2011 IEEE

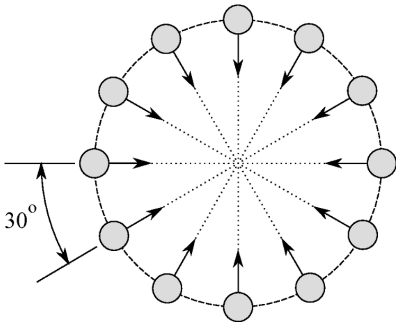

Fig. 2: The input is a circular spot of light (drawn to scale with respect to the size of the patch) moving from one end of the patch to the other in a straight line as shown, through the center of the retinal patch. Simulations are conducted for different angles from 0° to 330° at steps of 30°, with nine speeds for each direction. With the nine speeds used, the stimulus takes 0.4 to 2.0 seconds to cross the patch at steps of 0.2 seconds.

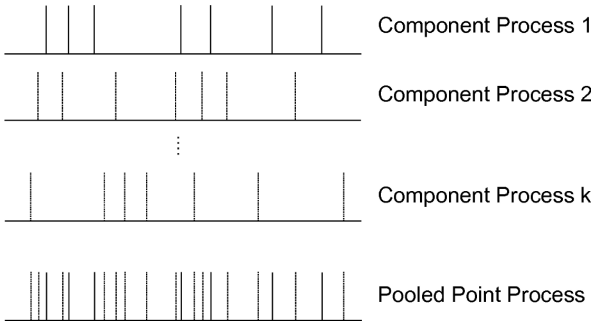

Fig. 3: An example of pooling spike events, demonstrated using three randomly chosen cells.

an inhomogeneous Poisson process (see [8], [9], [7]). An inhomogeneous Poisson process can be characterized by an intensity function $\lambda(t|\boldsymbol{v})$, which is a time ($t$) varying function In the experiments described in this paper, the input condition can be characterized by the velocity $\boldsymbol{v}$ of the motion target. The velocity has a magnitude v and an angle θ. In this paper we show that we can use the dependence of the intensity function on the speed and the direction of motion can be used to develop estimation algorithm.

II. Retinal Patch Model and Experimental Setup

As mentioned before, we use the retinal cell model described in the two conference papers, [6] and [7] as well as the PhD thesis [5]. The retinal cells were "sprinkled" over the retina to match the distributions given in [3] and [4]. Then, we selected a circular patch sampled from the center of the model retina as the model patch for these simulation experiments. The selected patch has a total of 520 cells, 54 A ON cells, 55 A OFF cells, and 134, 136 and 141 of the B cells sensitive to the direction of motion along 180°, 40° and -75° respectively.

In order to generate the patch response data, we considered a circular point light source on a dark background. The target size is one tenth of the patch size. The patch is taken to be the cells which are contained in a three millimeter circular disc centered at the location with maximum cell density on the visual streak. Nine speeds were used to study the statistical properties of the patch. The speeds of the spots were selected in such a way that the fastest speed will take 0.4 seconds of simulation time to traverse the patch. The subsequent speeds takes an extra 0.2 seconds to cross the patch, and at the slowest speed, the input takes two seconds to cross the patch. For each speed, twelve angles from 0° to 330°, equally spaced at 30° were used. Collectively, there are 108 different velocities, nine speeds each with twelve angles. For each velocity, the light spot starts from one end of the patch and goes to the other end of the patch through the center in a straight line (see Fig. 2). Each velocity is repeated sixty times. See Fig. 2 for a schematic of the input set up.

The model can be implemented on any compatible platform. However, in order to generate the data presented in this paper, we implement the filter cascade stage of the model on MATLAB [10] and the Hodgkin Huxley spiking neuron portion of the model is implemented on the GENESIS (*GE*neral *NE*ural *SI*mulation *S*ystem) neural simulator platform [11]. The responses of the GENESIS environment are saved as the time varying membrane potentials of each constituent cell of the patch. These voltage data is read in to and further processed in MATLAB. The spike times are identified by thresholding and detecting the rising edge of the thresholded voltage signal. We use these spike times as the data for our analysis.

III. Algorithms

A. Stochastic Process Model

The fundamental hypothesis of analysis is that the underlying point process of the spikes produced by the neurons is a self exciting point process (see [8], [9]). After pooling (see Fig. 3) the spiking activity of several cells (usually on a sub patch) we can model the resulting pooled process as an inhomogeneous Poisson process (see [8], [9]). We assume that the intensity function on the inhomogeneous Poisson process obtained by pooling has an intensity function $\lambda(t)$, which depends on the speed and the direction of motion. Thus we may write $\lambda(t) = \lambda(t|\boldsymbol{v})$ or $\lambda(t|v,\theta)$, where v is the speed, θ is the angle of motion and $\boldsymbol{v} = v\cos\theta\boldsymbol{i} + v\sin\theta\boldsymbol{j}$ is the velocity of the target. Here $\boldsymbol{i}$ and $\boldsymbol{j}$ are the unit vectors along the left to right and bottom to top, respectively. In other words, we assume that the response of the retinal patch due to the motion of a light spot with speed v at an angle θ is a realization of an inhomogeneous Poisson process with intensity $\lambda(t|v,\theta)$. Hence, the probability of having n spikes between the starting time 0 and arbitrary positive time t is given by

$$\Pr[N_{0,t} = n] = \frac{(\Lambda(t|v,\theta))^n}{n!}\exp\left(-\Lambda(t|v,\theta)\right), \qquad (1)$$

where $\Lambda(t|v,\theta) = \int_{\tau=0}^{t} \lambda(\tau|v,\theta)\ \mathrm{d}\tau$. We refer to $\lambda(\tau|v,\theta)$

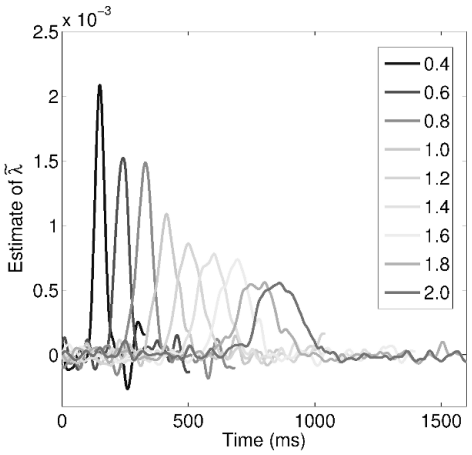

Fig. 4: Some estimates of $\tilde{\lambda}(t|v,\theta)$ as in (2) for a sub patch sampled from the center of the patch. The diameter of the sub patch is taken to be equal to the diameter of the light spot. Estimates shown for one instance of 0° for all the speeds. Legend is given in terms of the time the spot input takes to cross the patch.

as the the intensity function of the inhomogeneous Poisson process. We assume that the intensity function can be written as follows:

$$\lambda(t|v,\theta) = \lambda_0 + \tilde{\lambda}(t|v,\theta). \tag{2}$$

The first term λ_0, a constant term, which models the spikes due to the background noise of the retina. The second term $\tilde{\lambda}(t|v,\theta)$ is driven by the input stimulus parameterized by speed v and direction θ.

The first challenge of analyzing the retinal signals under this framework is to estimate the intensity function $\lambda(t|v,\theta)$. It is customary to estimate it using binning methods (see [12], [13], [14]). However, in our work we estimate $\Lambda(t|v,\theta)$ for each v and θ combination. First for each simulation, we obtain the cumulative spike count up to the time point t. Then this "cumulative spike count function" is averaged over all the repetitions of simulation for the selected v and θ. Then that "mean cumulative spike count function" is smoothed using a smoothing spline (it is possible to use a low pass filter as well but the details are not provided here). The resulting smooth function is claimed to be $\Lambda(t|v,\theta)$. When applying the smoothing algorithm, (spline or lowpass filtering) one should be careful to ensure that the $\Lambda(t|v,\theta)$ function is an increasing function, since we require $\lambda(t|v,\theta)$ to be non-negative. Furthermore, we can estimate the λ_0 term similarly by considering the response of the patch with no input incident on the retina. Once we obtain the estimates of $\lambda(t|v,\theta)$ for a particular v and θ, using the estimate of λ_0, we can calculate $\tilde{\lambda}(t|v,\theta)$ using (2). An example of the estimates of $\tilde{\lambda}(t|v,\theta)$ is shown in Fig. 4.

B. Speed Estimation

The speed estimates can be obtained by observing the half height pulse width (HHPW) of the $\tilde{\lambda}(t|v,\theta)$ function. We

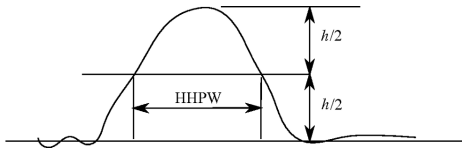

Fig. 5: Illustration of half height pulse width

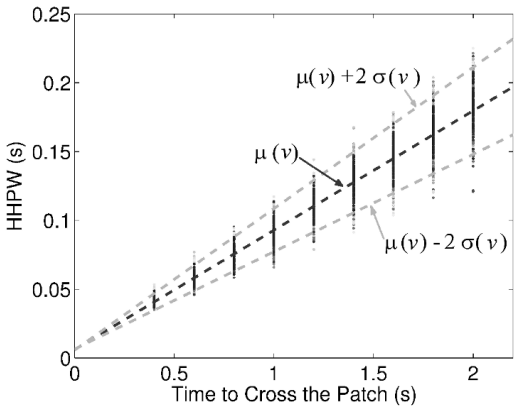

Fig. 6: Variation of half height pulse width with speed. The half height pulse width for the different speeds, over the different angle and multiple simulations plotted with the time the input stimulus takes to cross the patch (the "vertical line segments" are actually dots representing the half height pulse width at each speed). Due to the large number of points per speed, it appears like a line segment. The variation of mean $\mu(v)$ and standard deviation $\sigma(v)$ are also shown on the graph. Note that the mean and standard deviation vary linearly with the time the spot input takes to cross the patch showing that the mean and standard deviation are inversely proportional to the speed of the input. Also note that the most of the data points fall within the lines $\mu(v) \pm \sigma(v)$, where $\mu(v)$ and $\sigma(v)$ are respectively the linear regressions of mean and standard deviation of half power pulse width with speed.

define half height pulse width to be the width of the $\tilde{\lambda}(t|v,\theta)$ function at half its maximum value (see 5). The half height pulse width is a good measure of pulse width of a pulse-like signal we have for $\tilde{\lambda}(t|v,\theta)$. From Fig. 4, it is clear that for faster speed (when the light spot crosses the patch in a shorter time) $\tilde{\lambda}(t|v,\theta)$ is narrower than for slower speed (when the light spot takes a longer time to cross the patch)

From Fig. 6 we can see that it is possible to perform a linear regression between the mean $\mu(v)$ and the time the input takes to cross the patch. Similarly, we can perform another linear regression with standard deviation $\sigma(v)$ and the time the input takes to cross the patch. Note that most of the data points fall within the two lines $\mu(v) \pm \sigma(v)$ in Fig. 6. Furthermore, assuming Gaussian distribution for the variation of half height pulse width for a particular speed, we can write the likelihood function as a function of speed. Therefore, given a response from the model patch,

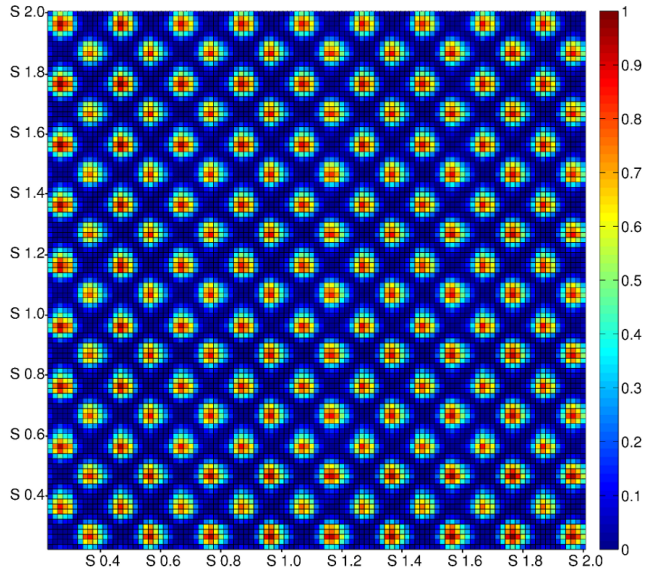

Fig. 7: The normalized $\mathcal{L}^2$ distance between the intensity functions after linearly rescaling the time to a standard $[0, 1]$ time interval. Both horizontal and vertical axis contain the angles 0° to 330° at steps of 30° for the different speeds (denoted by the time to cross the patch). For example, between 'S 0.4' and 'S 0.6', we have the twelve different angles corresponding to the speed for which the stimulus takes 0.6 seconds to cross the patch.

we can estimate the speed of the target. Under the Gaussian hypothesis, the likelihood function (see [15]) is:

$$L(v|r) = \frac{\exp\left(-(r-\mu(v))^2/2\sigma^2(v)\right)}{\sqrt{2\pi\sigma^2(v)}}. \qquad (3)$$

Then, given an observation (i.e. the half height pulse width) the task will be to find the speed v that will maximize the likelihood function $L(v|r)$. This is possible because we can find a relation between mean, standard deviation and speed.

C. Rescaling and Estimation of Motion Direction

In our previous work, we have shown that the turtle retina can encode the direction of motion of a target if the speed is fixed and known. In the analysis using the model of the turtle retina, it was found that there are certain features of the retinal response which are preserved under different speeds, but unique to a certain direction of motion.

Suppose that for a particular speed v and angle θ combination the light input takes $T_{v,\theta}$ seconds to cross the patch. Then, the idea proposed in this paper is to linearly rescale the time to a standard $[0, 1]$ time interval and study the common features of the variation of the intensity function in the rescaled time. Fig. 7 shows that the variation of the intensity function is 'fairly close' in terms of the $\mathcal{L}^2$ norm after rescaling. This is a good indication that we may be able to discriminate the angle of motion of the input stimulus using the variation of the intensity function in linearly rescaled time.

Principal Component Analysis (PCA) also known as the discrete Karhunen Loeve transform (KLT) (see [16]) can be effectively used to represent a high dimensional data (such as the intensity function, which is infinite dimensional) as points in a lower dimensional space. Therefore, principal component analysis has been a popular method for analyzing neural signals from large populations of neurons (see [17], [18], [19], [7]).

Once the intensity functions (for the entire patch or a smaller sub patch) is obtained, we can project them on to a lower dimensional (usually three dimensions for display purposes, higher dimensions for other calculations) space. The principal component points can be assumed and verified to (using the Lilliefors [20] test or Kolmogorov-Smirnov (KS) test [21]) be realizations of a multivariate normal distribution. Using mean $\boldsymbol{\mu}_\theta = \boldsymbol{\mu}(\theta)$ and $\Sigma_\theta = \Sigma(\theta)$ obtained experimentally, we can write the likelihood function (see [15]), given the k-dimensional observation $\boldsymbol{r}$ from the principal component space to be as follows:

$$L(\theta|r) = \frac{\exp\left(-(\boldsymbol{r}-\boldsymbol{\mu}_\theta)^\top \Sigma_\theta (\boldsymbol{r}-\boldsymbol{\mu}_\theta)/2\right)}{\sqrt{2^k\pi^k\,|\Sigma_\theta|}}. \qquad (4)$$

Here again we need to find θ such that $\boldsymbol{\mu}_\theta$ and Σ_θ will maximize $L(\theta|r)$, and that θ will be the maximum likelihood estimate corresponding to the observation r (see [15]). However, unlike in the case of the speed estimation problem above, we do not have a clear simple relation between the motion direction θ and $\boldsymbol{\mu}_\theta$ and Σ_θ. Therefore, we can only perform a discrimination of the motion direction given the observation.

When we take the principal components corresponding to the response of the whole patch, the principal component points cluster together. This results in a poor estimation performance, in terms of the root mean square error. However, if we look at the probability of error or the mean square error from each sub patch (see Fig. 8), we can see that the motion directions which cross a particular sub patch has a lesser probability of error. The overall probability of error on a sub patch is less than 0.5, as can be seen in Fig. 9 We can use this fact to reduce the detection error by using a 'voting' method (see [22], [23]) over the sub patches. In the voting method, we would claim that a particular angle θ is the estimate if the majority of the sub patches detect θ to be the maximum likelihood estimate.

IV. Results

A. Estimating Speed

As shown in Fig. 6, it is possible to establish a linear relation with the time the spot takes to cross the patch and the half height pulse width. Therefore, we can use the likelihood function (3) to estimate the speed of the moving target. Fig. 10 shows the variation of the relative error

$$\text{Relative Error} = \frac{|\text{Actual Speed} - \text{Estimated Speed}|}{\text{Actual Speed}}. \qquad (5)$$

The relative error can be expressed in terms of the time the light stimulus takes to cross the patch. Let T_{EST} is the

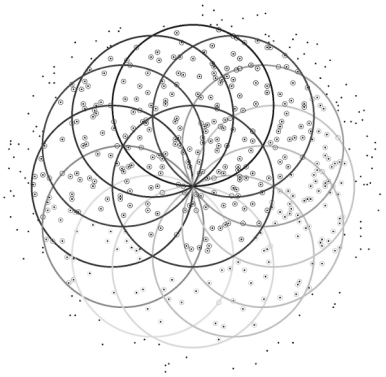

Fig. 8: Selection of sub patches from the retinal patch. The diameter of the sub patches are approximately one third of the diameter of the retinal patch. The sub patch in the middle is centered at the center of the retinal patch. The twelve surrounding sub patches are symmetrically located with the centers on the circumference of the sub patch in the middle.

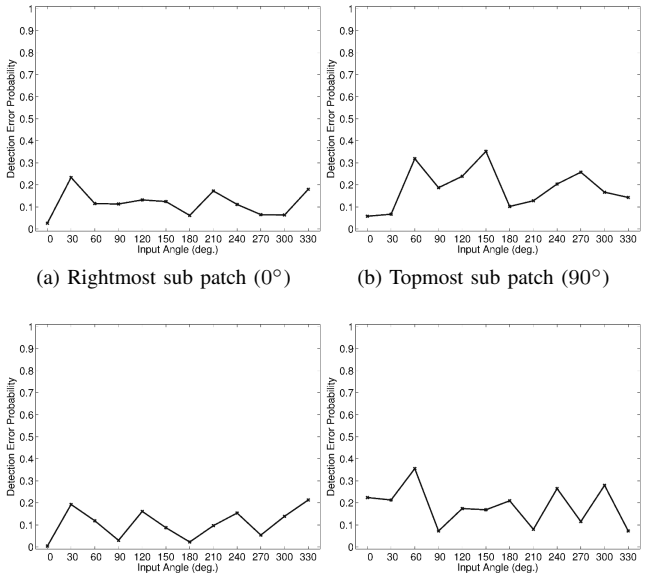

(a) Rightmost sub patch (0°) (b) Topmost sub patch (90°)

(c) Leftmost sub patch (180°) (d) Bottom sub patch (270°)

Fig. 9: Probability of error with sub patches. Shows the variation of the error probability of detection using four different sub patches.

estimate (using the half height pulse width) and T_{ACT} is the actual time to cross the patch with diameter d. Then the speed estimate is d/T_{EST} and the actual speed is d/T_{ACT}. Now we can write the relative error in speed estimate as follows:

$$\text{Relative Error} = \frac{|T_{EST} - T_{ACT}|}{T_{EST}}. \tag{6}$$

Fig. 11 shows the variation of relative root mean square error. It can be seen that the relative error is constant. The higher speeds, signified by shorter time to cross the patch, has a slightly less relative error of estimation. Overall, the relative error is about 0.1, i.e. 10%. Therefore, it is possible to estimate the speed with a reasonable accuracy. We should note that this is an estimation problem, not a discrimination problem.

B. Estimating the Direction of Motion

If we pool retinal cell spiking of the entire retinal patch or if we only use one sub patch, the estimation of the motion direction using the rescaled intensity functions becomes hard due to the large variance. However, most of the time we are able to discriminate the angle using the linearly time rescaled signal. For most of the angles, the root mean square error is between 20° and 40°, which is very close to the difference between the angles, 30°.

However, the 'voting' method yields far superior results. With the voting method, the probability of error will be almost zero. Hence no result graphs are shown in this paper. Over the pool of test angles used, the voting method was able to classify the correct angle estimate 539 times out of the 540 trials considered.

V. Conclusion

In this paper we present the details of a study on estimating motion parameters using the responses of a turtle retina using a mathematical model. In particular, we present the results on two of our current studies. First, on estimating the speed of a target which is moving along an unknown but fixed direction, and the second, on discriminating the direction of motion of a target moving with an unknown yet fixed speed.

We propose an algorithm using the intensity function of the spiking process, motivated by the theory of point processes. We can represent the intensity function of the underlying inhomogeneous Poisson process as the sum of two terms: first, a constant term representing the background noise and second, the signal dependent term. We can estimate the integral of the intensity function under the Poisson assumption, using the cumulative sum of the spike count of the whole patch or a sub patch under the study.

We present two main concepts with respect to the two problems we study in this paper. The first main concept is that we can estimate the speed using the half height pulse width of the intensity function. In Fig. 11 we can see that the speed can be estimated within, on average, 10% of the exact value.

The other main concept is the idea of rescaling the time linearly to a standard value and using the resulting intensity function to estimate the direction of motion. From Fig. 7, there is a clear difference between the intensity function estimates due to the different direction of motion of the light input after rescaling every thing to a standard time. However, the time rescaled intensity functions vary significantly due to system noise. Hence the estimation of angles using the time rescaled intensity functions is not an easy task. By subtracting the estimate of the background noise, the performance can be improved. But still there is a lot of variability in the intensity function. The maximum likelihood

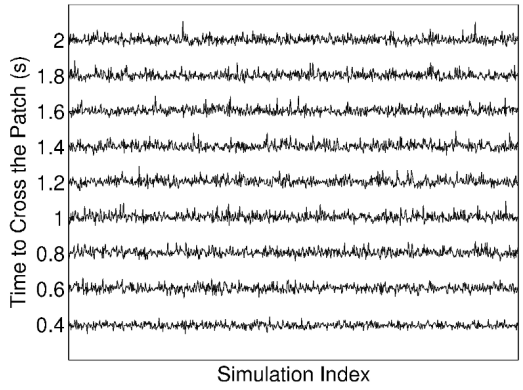

Fig. 10: The variation of relative estimation error of speed over the collection of simulations. The horizontal axis gives the simulation index. For any given speed, we have twelve angles and for each angle–speed combination, there are sixty simulations. So, in this speed estimation experiment, there are 720 simulations 12×60 trials each. The vertical axis is subdivided in to the different speeds, indicated by the time the stimulus takes to cross the patch. For, each speed, the relative estimation error is plotted, with the simulation index.

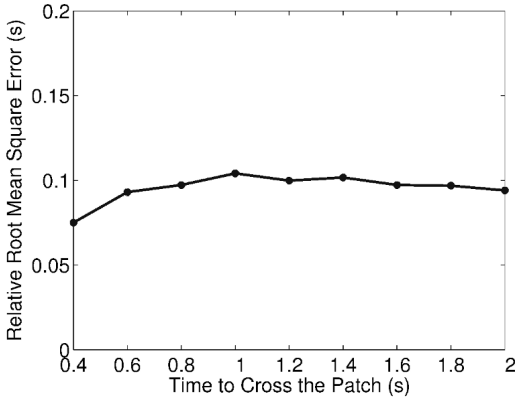

Fig. 11: Root mean square of the relative error of the speed estimates over the different speeds. The relative root mean square error is steady over the slower speeds (longer time to cross the patch). The relative error of estimates of the higher speeds are slightly less but not significantly different.

estimation over the principal component points does not give a good estimation result. With principal component analysis and maximum likelihood estimation, together with the voting method over the sub patches, it is possible to achieve almost perfect detection.

The Poisson process model opens up the possibility of applying maximum likelihood methods for inhomogeneous Poisson processes in [8], [9] as well as filtering methods with the framework of 'doubly stochastic' Poisson processes as described in [24], [8]. These methods will be explored in the future.

REFERENCES

[1] D. B. Bowling, "Light responses of ganglion cells in the retina of the turtle," *Journal of Physiology*, vol. 299, pp. 173–196, February 1980.

[2] P. L. Marchiafava and R. Weiler, "Intracellular analysis and structural correlates of the organization of inputs to ganglion cells in the retina of the turtle," *Proceedings of the Royal Society of London. Series B, Biological Sciences*, vol. 208, no. 1170, pp. 103–113, June 1980.

[3] E. H. Peterson and P. S. Ulinski, "Quantitative studies of retinal ganglion cells in a turtle, pseudemys scripta elegans I: Number and distribution of ganglion cells," *Journal of Comparative Neurology*, vol. 186, pp. 17–42, 1979.

[4] ——, "Quantitative studies of retinal ganglion cells in a turtle, pseudemys scripta elegans II: Size spectrum of ganglion cells and its regional variation," *Journal of Comparative Neurology*, vol. 208, pp. 157–168, 1982.

[5] M. P. B. Ekanayake, "Motion encoding and decoding in the turtle retina," Ph.D. dissertation, Department of Mathematics and Statistics, Texas Tech University, Lubbock, TX 79409, USA., July 2011.

[6] B. K. Ghosh, M. P. B. Ekanayake, and P. S. Ulinski, "Motion encoding and decoding in the turtle retina," *Proceedings on the European Control Conference, Budapest, Hungary*, August 2009.

[7] M. P. B. Ekanayake and B. K. Ghosh, "Detection of motion direction using a model of turtle retinal patch," *Proceedings of the IFAC World Congress, Milano, Italy*, August 2011.

[8] D. Snyder, *Random Point Processes*. John Wiley & Sons Inc., November 1975.

[9] D. L. Snyder and M. I. Miller, *Random Point Processes in Time and Space*, ser. Springer Texts in Electrical Engineering, J. B. Thomas, Ed. Springer-Verlag, 1991.

[10] MathWorks, "Matlab," 2009. [Online]. Available: http://www.mathworks.com/products/matlab/

[11] J. M. Bower and D. Beeman, *The Book of GENESIS: Exploring Realistic Neural Models with GEneral NEural SImulation System*, 2nd ed. Springer Telos, 1998.

[12] E. N. Brown, R. C. Barbieri, V. Ventura, R. E. Kass, and L. M. Frank, "The time-rescaling theorem and its applications to neural spike train data analysis," *Neural Computation*, vol. 14, pp. 325–346, 2001.

[13] U. T. Eden, L. M. Frank, R. C. Barbieri, V. Solo, and E. N. Brown, "Dynamic analysis of neural encoding by point process adaptive filtering," *Neural Computation*, vol. 16, no. 5, pp. 971–998, May 2004.

[14] A. R. C. Paiva, "Reproducing kernel Hilbert spaces for point processes, with applications to neural activity analysis," Ph.D. dissertation, University of Florida, 2008.

[15] H. L. Van Trees, *Detection, Estimation and Modulation Theory, Part I*. John Wiley & Sons Inc., 1968.

[16] I. T. Jolliffe, *Principal Component Analysis*, 2nd ed., ser. Springer Series in Statistics. Springer, 2002.

[17] Z. Nenadic, B. K. Ghosh, and P. S. Ulinski, "Modeling and estimation problems in the turtle visual cortex," *IEEE Transactions in Biomedical Engineering*, vol. 49, no. 8, pp. 753–762, August 2002.

[18] X. Du, B. K. Ghosh, and P. S. Ulinski, "Encoding and decoding target locations with waves in the turtle visual cortex," *IEEE Transactions in Biomedical Engineering*, vol. 52, no. 4, pp. 566–577, April 2005.

[19] ——, "Encoding of motion targets by waves in the turtle visual cortex," *IEEE Transactions in Biomedical Engineering*, vol. 53, no. 8, pp. 1688–1695, August 2006.

[20] H. Lilliefors, "On the Kolmogorov–Smirnov test for normality with mean and variance unknown," *Journal of the American Statistical Association*, vol. 62, pp. 399–402, June 1967.

[21] F. J. Massey, "The Kolmogorov-Smirnov test for goodness of fit," *Journal of the American Statistical Association*, vol. 46, no. 253, pp. 68–78, 1951.

[22] S. Theodoridis and K. Koutroumbas, *Pattern Recognition*, 4th ed. Academic Press, 2009.

[23] L. Lam and C. Y. Suen, "Application of majority voting to pattern recognition: An analysis of its behavior and performance," *IEEE Transactions on Systems, Man and Cybernetics - Part A: Systems and Humans*, vol. 27, no. 5, pp. 553–568, 1997.

[24] D. Snyder, "Filtering and detection for doubly stochastic poisson processes," *IEEE Transactions on Information Theory*, vol. 18, no. 1, pp. 91–102, 1972.